

Angular distributions of γ rays from the ${}^7\text{Li}(p,\gamma)$ reaction at low energies

K. I. Hahn, C. R. Brune, and R. W. Kavanagh

W. K. Kellogg Radiation Laboratory, California Institute of Technology, Pasadena, California 91125

(Received 1 November 1995)

Angular distributions of the 14–17 MeV γ rays from the ${}^7\text{Li}(p,\gamma)$ reaction at $E_p=450$, 402, and 80 keV were measured at $0^\circ \leq \theta_{\text{lab}} \leq 135^\circ$, using a BGO detector and a $28\text{-}\mu\text{g}/\text{cm}^2$ LiF target. The angular distributions at $E_p=450$ and 402 keV agree with the previous results by Mainsbridge; at $E_p=80$ keV the ground-state transition is anisotropic on the order of 20%, confirming recent results by Chasteler *et al.*

PACS number(s): 25.40.Lw, 27.20.+n

I. INTRODUCTION

A recent report [1] of significant γ -ray anisotropy and analyzing power in the ${}^7\text{Li}(p,\gamma)$ reaction at $E_p \leq 80$ keV deduced a considerable p -wave contribution (18–95 %) and a lower extrapolated zero-energy S factor than previously reported. Chasteler *et al.* suggested a similar effect for the p -wave contribution to the ${}^7\text{Be}(p,\gamma)$ reaction at low energies, which reduces the $S(E)$ factor considerably and thus decreases the solar-model flux of high-energy solar neutrinos. This suggestion has been criticized by Barker [2] in a detailed theoretical analysis.

The anisotropy of the ${}^7\text{Li}(p,\gamma)$ reaction measured by Chasteler *et al.* is $\sim 20\%$, in disagreement with the previous experiment by Cecil *et al.* [3], who reported isotropy within 10%. Mainsbridge [4] measured angular distributions at higher energies, $200 \leq E_p \leq 1100$ keV. Our results for angular distributions of the ${}^7\text{Li}(p,\gamma)$ reaction measured at three proton energies are discussed in the following sections.

II. EXPERIMENTAL SETUP

Beams with intensities of 10–30 μA (H_3^+) for $E_p=80$ keV and 1–2 μA (protons) for both $E_p=402$ keV and $E_p=450$ keV were produced by the Caltech Pelletron accelerator. The beams were rastered magnetically to sweep over the area of a 6-mm \times 17-mm aperture ~ 1 m before the target. We used the same detectors and the target holder developed for a previous experiment [5] as shown in Fig. 1. The γ rays from the ${}^7\text{Li}(p,\gamma)$ reaction were measured with a 5.08-cm-length \times 5.08-cm-diam BGO detector and a 7.62-cm-length \times 7.62-cm-diam NaI detector. The front face of the BGO detector was positioned at 7.62 cm from the center of the target for the $E_p=402$ and $E_p=450$ keV runs, and 3.81 cm for the $E_p=80$ keV run. The BGO detector was rotated in the horizontal plane between 0° and 135° , with a 15° interval, with respect to the incident beam. The NaI detector positioned at 3.81 cm was used to normalize the BGO yields. For the 80-keV run, a 2.54-cm-thick and $63.5 \times 58.4\text{-cm}^2$ -area plastic scintillator placed above both detectors was used to veto cosmic rays in order to reduce background.

A $28\text{-}\mu\text{g}/\text{cm}^2$ target of ${}^{\text{nat}}\text{LiF}$ (92.5% ${}^7\text{Li}$), evaporated onto a 0.81-mm-thick Cu backing, was mounted at 45° with respect to the incident beam and was water cooled. The

“positive” side (as labeled in Fig. 1) was used for runs with the BGO detector at $\theta \leq 90^\circ$, whereas the “negative” side was used for runs at $\theta \geq 90^\circ$, in order to avoid the large corrections due to the absorbers at certain angles, for example, $\theta = +135^\circ$ and $\theta = -45^\circ$. The two 90° runs were used to normalize other angles. Using the S factors for the ${}^7\text{Li}(p,\gamma){}^8\text{Be}$ reaction measured by Zahnow *et al.* [6], the cross-section-weighted energies within the target are $E_{\text{eff}}=442$ and 396 keV for $E_p=450$ and 402 keV, respectively. At $E_p=80$ keV, the proton energy loss in the target was 21 keV, and $E_{\text{eff}}=73$ keV (the same as for the thick Li target used by [1]).

Because we depend exclusively on Monte Carlo calculations for the (relative) γ -ray detection efficiencies at various angles, it is important to test the program, EGS4 [7], in our asymmetric-absorption geometry. Accurate dimensions and elemental composition of the target and detector system were determined as input for the program. In a previous test [5] using the 6.13-MeV γ rays from ${}^{19}\text{F}(p,\alpha\gamma){}^{16}\text{O}$, the absolute efficiency from EGS4 was found accurate to within 6%.

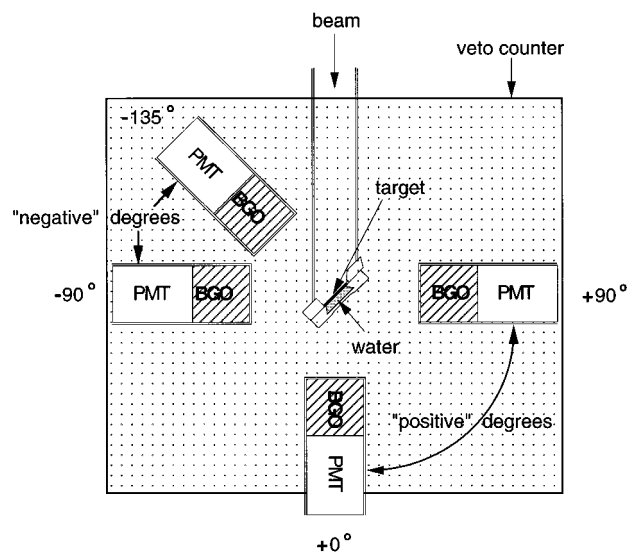


FIG. 1. Schematic of the experimental setup, showing the target and some of the positions of the BGO detector. The NaI detector (not shown here) was positioned at “negative” 90° and “positive” 90° for BGO runs at “positive” angles and “negative” angles, respectively.

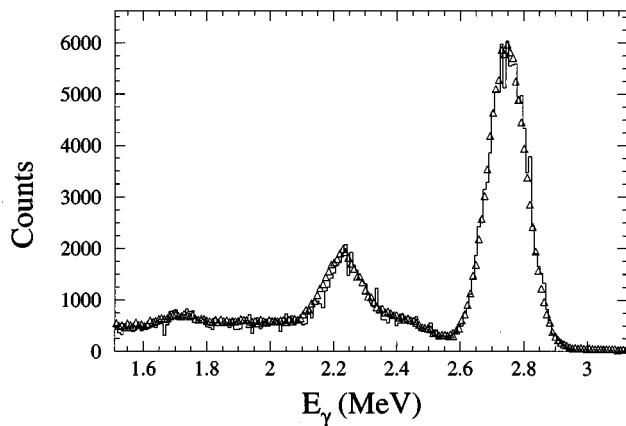


FIG. 2. The experimental (triangles) and the Monte Carlo (histograms) spectra for the 2.75-MeV γ 's from ^{24}Na are compared. The energy spectrum from the Monte Carlo simulation was smeared with $\sim 5\%$ energy resolution to match the experimental data of the BGO detector.

Here, to test the angular dependence, we produced a ^{24}Na radioactive source of 2.75-MeV γ rays that accurately simulated the geometry used for $^7\text{Li}(p, \gamma)$.

III. ANGULAR DISTRIBUTION OF ^{24}Na γ RAYS

A 1-mg/cm²-thick Na_2WO_4 target on a 0.81-mm-thick Cu backing was bombarded for 50 min by a 2.1-MeV deuteron beam of 1.0–1.5 μA , rastered and collimated as for our $^7\text{Li}(p, \gamma)$ experiment. From the $^{23}\text{Na}(d, p)$ reaction, ^{24}Na is produced in the target, distributed according to the rastering, and emitting γ rays isotropically. A thin Au layer, evaporated onto the surface, prevented loss of ^{24}Na during the production run. After a 1-day wait for the activity to decay to a suitable level, spectra from the BGO (at 7.62 cm) were taken at various angles (between 0° and 135° with a 15° interval). Figure 2 shows the experimental data (triangles) of the BGO detector at -90° and the corresponding Monte Carlo spectrum (histogram), which was convolved with energy resolution of 5% to fit the shapes of the experimental spectra. The relative raw and corrected γ yields, normalized to the 90°

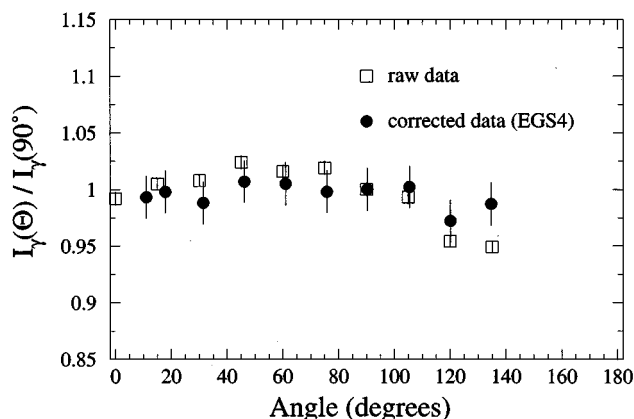


FIG. 3. The relative yields normalized to the 90° yields are plotted for the raw experimental data, and the corrected data using EGS4, for the ^{24}Na source.

yields, are plotted in Fig. 2. In view of the 45° target holder, and the beam pipe at backward angles, the raw yields behaved as expected; for example, for $0^\circ \leq \theta \leq 90^\circ$, the raw yields are expected to be maximum at 45° and symmetric about the 45° line, and for $90^\circ \leq \theta \leq 135^\circ$, the raw yields decrease when the detector angle increases.

The yield at the “positive” 90° , as indicated in Fig. 1, was used to normalize the yields at $<90^\circ$, and the yield at the “negative” 90° was used to normalize the yields at $>90^\circ$. The relative yields have then to be corrected for the angle-dependent absorption losses. For example, due to absorptions of the Cu backing, the stainless-steel (SS) target holder, and cooling water, the loss at $\theta_{\text{lab}} = 0^\circ$ is larger than at $\theta_{\text{lab}} = 135^\circ$, where there is only the SS beam pipe (0.318-cm wall thickness).

The raw γ yields are corrected for the half-life of ^{24}Na , $t_{1/2} = 14.96$ h, but not for different absorption coefficients and detector angles due to the finite size of the BGO detector. These latter corrections were calculated using EGS4, with results as shown in Fig. 3. The errors of the corrected yields include the statistical errors of the total counts in the Monte Carlo calculations and the experimental γ counts, and 1.5% systematic errors, which are mainly due to the uncertainty in the detector distance. The angular distribution of the corrected yields is isotropic within the experimental errors, giving confidence in the use of the Monte Carlo simulations for the $^7\text{Li}(p, \gamma)$ case.

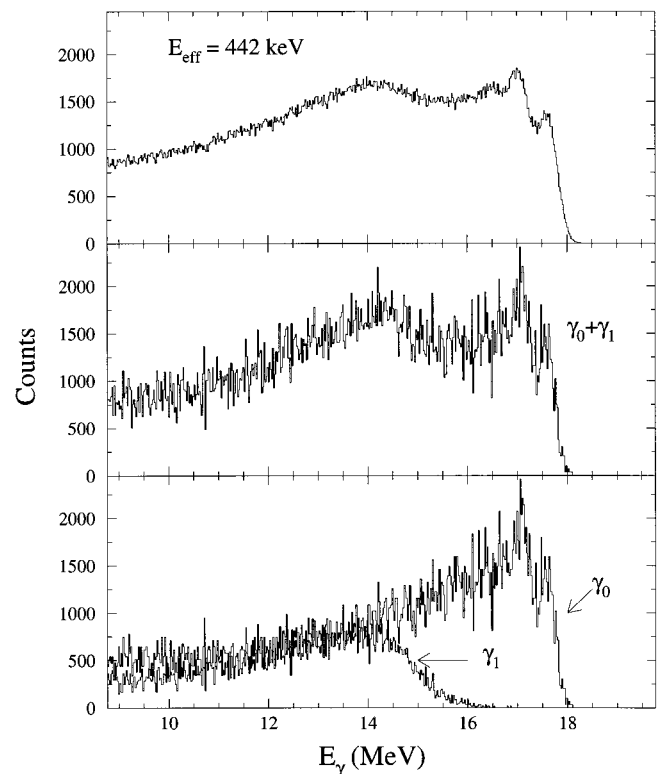


FIG. 4. The top spectrum shows the (background-subtracted) experimental data of the BGO detector for the $^7\text{Li}(p, \gamma)$ reaction at $E_{\text{eff}} = 442$ keV, $\theta = 90^\circ$. The middle and bottom spectra are the Monte Carlo results. The ratio $\gamma_0 / (\gamma_0 + \gamma_1) = 0.74 \pm 0.03$.

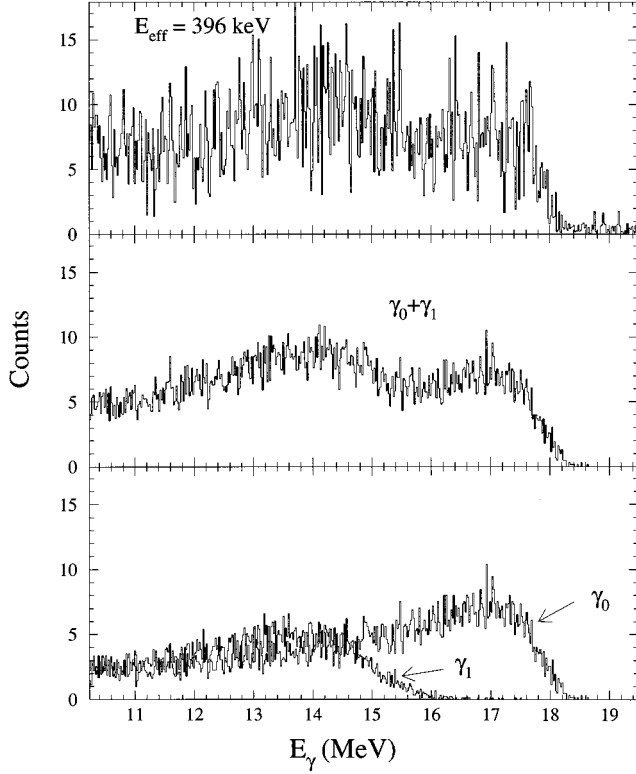


FIG. 5. The top spectrum shows the (background-subtracted) experimental data of the BGO detector for the ${}^7\text{Li}(p, \gamma)$ reaction at $E_{\text{eff}} = 396$ keV, $\theta = 90^\circ$. The middle and bottom spectra are the Monte Carlo results. $\gamma_0 / (\gamma_0 + \gamma_1) = 0.41 \pm 0.03$.

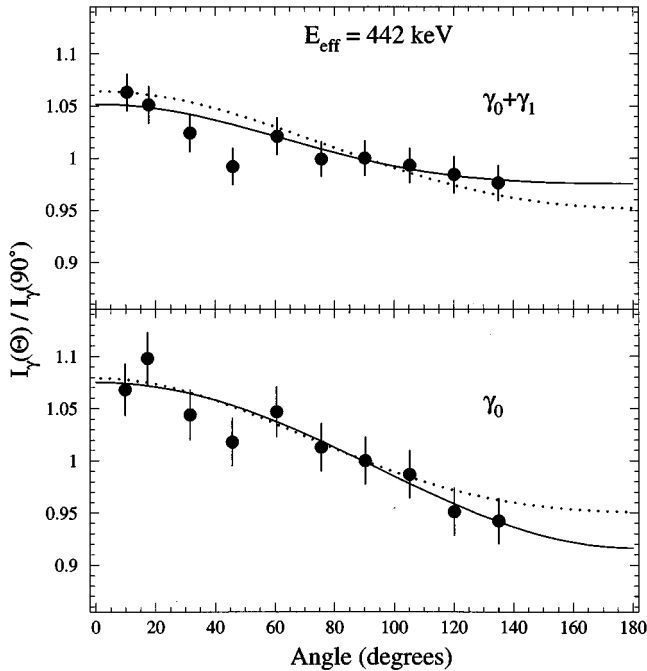


FIG. 6. The relative yields normalized to the 90° yields are plotted for the ${}^7\text{Li}(p, \gamma)$ reaction at $E_{\text{eff}} = 442$ keV. The solid lines are fits to our data (points) and the dotted lines are from Mainsbridge.

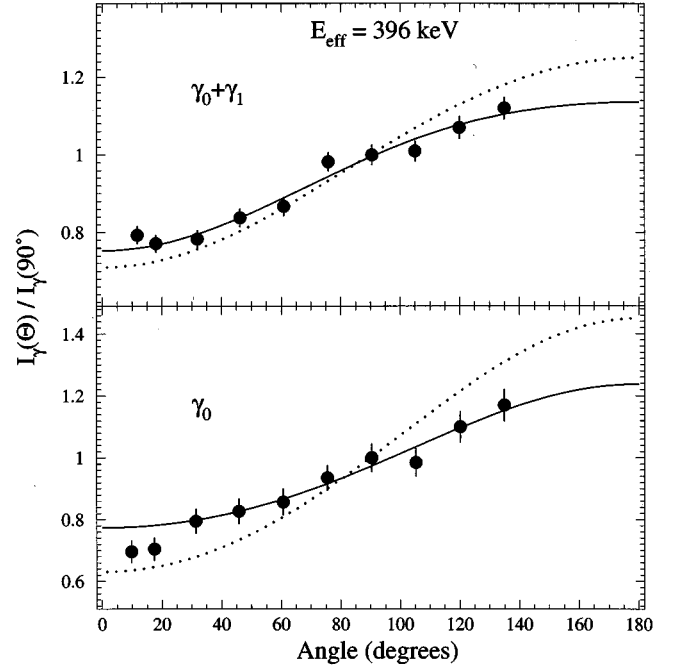


FIG. 7. The relative yields normalized to the 90° yields are plotted for the ${}^7\text{Li}(p, \gamma)$ reaction at $E_{\text{eff}} = 396$ keV. The solid lines are fits to our data (points). The dotted lines are from Mainsbridge.

IV. EXPERIMENTAL PROCEDURES AND RESULTS

Our main objective was to measure the angular distribution of the γ rays from the ${}^7\text{Li}(p, \gamma)$ reaction at $E_p \leq 80$ keV, because the 20% anisotropy measured in the recent experiment [1], which plays an important role in determining the p -wave contribution, is in disagreement with the previous experiment [3]. We also measured angular distributions at the higher energies, 442 and 396 keV, in order to compare with Mainsbridge.

As for the ${}^{24}\text{Na}$ case, we used the EGS4 code to calculate the efficiencies at various angles as well as the effective angles due to finite detector size. For the forward angles, the main absorbers (the Cu backing, water, the target holder) are symmetric about 45° . Our EGS4 results confirm this, as the calculated absorptions at 0° , 15° , and 30° , agree with those at 90° , 75° , and 60° , respectively, within 3% statistical errors.

In the Monte Carlo calculations, for each proton energy, one million γ_0 rays and one million γ_1 rays, from the ${}^7\text{Li}(p, \gamma_0){}^8\text{Be}(\text{g.s.})$ and ${}^7\text{Li}(p, \gamma_1){}^8\text{Be}^*(3.04\text{-MeV})$ reactions, respectively, on the $6\text{-mm} \times 17\text{-mm}$ target area were generated isotropically. The width of the 3.04-MeV state in ${}^8\text{Be}$, $\Gamma_{\text{c.m.}} = 1500 \pm 20$ keV [8], exceeds the detector resolution, and we used the shape and width of the state from [9] for the γ_1 calculations. The good statistics for the γ rays observed at the 442-keV resonance enabled us to study the shape of the spectrum in the BGO detector and to compare with the Monte Carlo simulations used to separate the γ_0 's from the γ_1 's. The γ -ray energies in the laboratory system were corrected for recoil energy and Doppler shift and their energies deposited in the BGO crystal were determined.

A typical spectrum of the γ rays from the ${}^7\text{Li}(p, \gamma)$ reaction at $E_{\text{eff}} = 442$ keV is shown in the top of Fig. 4. The

TABLE I. Values of the Legendre coefficients of the fits for Figs. 5, 7, and 9.

E_{eff} (keV)	$\gamma_0 + \gamma_1$			γ_0		
	A_0	A_1	A_2	A_0	A_1	A_2
442	1.003 ± 0.007	0.038 ± 0.015	0.010 ± 0.018	0.998 ± 0.009	0.079 ± 0.019	-0.002 ± 0.024
396	0.978 ± 0.011	-0.191 ± 0.021	-0.033 ± 0.035	0.983 ± 0.019	-0.232 ± 0.036	0.022 ± 0.057
73	1.001 ± 0.012	-0.086 ± 0.022	-0.005 ± 0.031	1.084 ± 0.021	-0.179 ± 0.043	

Monte Carlo results shown in the middle spectrum of Fig. 4 accurately predict the shape and peak positions of the experimental data shown in the top spectrum. The bottom spectrum shows the Monte Carlo simulation for γ_0 and γ_1 separately, and indicates that γ_0 events dominate above 16 MeV. Similarly, Fig. 5 shows the experimental data and the Monte Carlo results for the ${}^7\text{Li}(p, \gamma)$ reaction at $E_{\text{eff}} = 396$ keV.

The solid lines in Figs. 6 and 7 are least-squares fits by an expansion in Legendre polynomials of the form, $A_0 + A_1 P_1(\cos\theta) + A_2 P_2(\cos\theta)$, to our experimental (EGS4 corrected) results for $0^\circ \leq \theta \leq 135^\circ$. Higher-order terms were not required to fit the data. The values of the coefficients of the angular distributions in Figs. 6 and 7 are shown in Table I. The results for the angular distributions at $E_{\text{eff}} = 442$ keV and $E_{\text{eff}} = 396$ keV are in reasonable agreement with the results by Mainsbridge [4], shown as dotted lines.

Figure 8 shows the γ spectrum from the ${}^7\text{Li}(p, \gamma)$ reaction at $E_{\text{eff}} = 73$ keV. Errors in Fig. 9 are largely due to the

statistical errors of the total γ counts as well as 1.5% systematic errors for the uncertainties in the detector position. The solid lines in Fig. 9 are the results of least-squares fits to the experimental data. The coefficients are listed in Table I. Our fit to the γ_0 angular distribution, which indicates $\sim 20\%$ anisotropy, agrees well with the results of Chasteler *et al.*

V. CONCLUSION

Our results for the angular distributions of the ${}^7\text{Li}(p, \gamma)$ reaction at $E_{\text{eff}} = 442$ keV and $E_{\text{eff}} = 396$ keV agree with the previous results by Mainsbridge within errors. They also agree well with the forward-backward asymmetries, $I(0^\circ)/I(150^\circ)$, recently reported by Zahnow *et al.* [6] We have measured angular distributions of both γ_0 and the sum, $\gamma_0 + \gamma_1$, at $E_{\text{eff}} = 73$ keV. Our results for γ_0 at $E_{\text{eff}} = 73$ keV are in good agreement with the results by Chasteler *et al.*, but disagree with the isotropy reported by Cecil *et al.* Barker

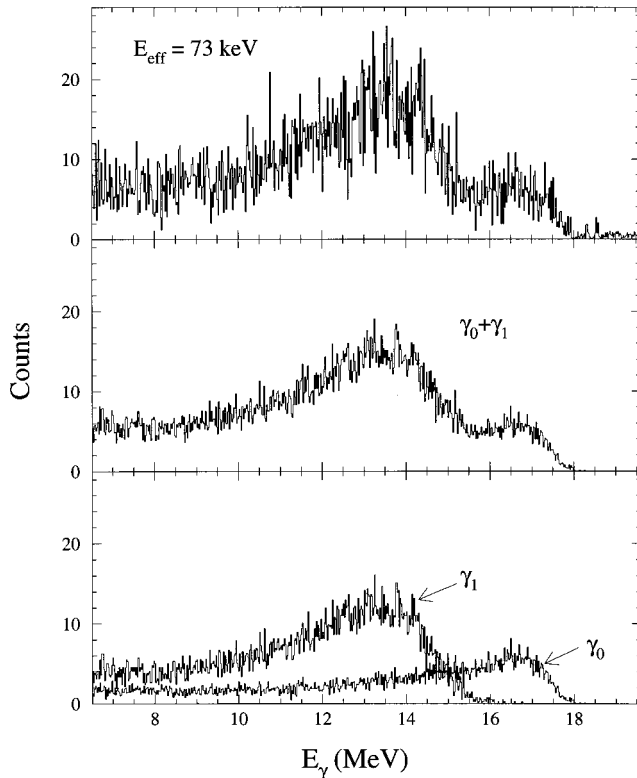


FIG. 8. The top spectrum shows the (background-subtracted) experimental data of the BGO detector for the ${}^7\text{Li}(p, \gamma)$ reaction at $E_{\text{eff}} = 73$ keV, $\theta = 90^\circ$. The middle and bottom spectra are the Monte Carlo results. $\gamma_0/(\gamma_0 + \gamma_1) = 0.29 \pm 0.03$.

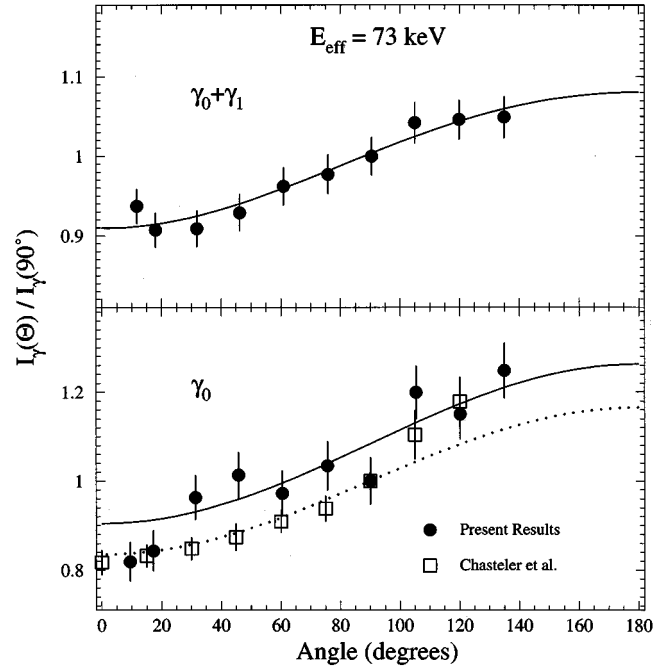


FIG. 9. The relative yields normalized to the 90° yields are plotted for our results ($\gamma_0 + \gamma_1$ and γ_0) and Chasteler *et al.* (γ_0) for the ${}^7\text{Li}(p, \gamma)$ at $E_{\text{eff}} = 73$ keV. The solid lines are fits to our results. The dotted line in the bottom spectrum is the fit to our results, normalized to unity average.

[2] has shown that acceptable theoretical fits to the low-energy angular-distribution and analyzing-power data [1] can be obtained by attributing the p -wave $M1$ contributions to the tails of the higher resonances at $E_p=441$ and 1030 keV.

ACKNOWLEDGMENT

This work was supported in part by the National Science Foundation Grant No. PHY94-20470.

-
- [1] R. M. Chasteler, H. R. Weller, D. R. Tilley, and R. M. Prior, Phys. Rev. Lett. **72**, 3949 (1994).
[2] F. C. Barker, Aust. J. Phys. **48**, 813 (1995).
[3] F. E. Cecil, D. Ferg, H. Liu, J. C. Scorby, and J. A. McNeil, Nucl. Phys. **A539**, 75 (1992).
[4] B. Mainsbridge, Nucl. Phys. **21**, 1 (1960).
[5] K. I. Hahn, C. R. Brune, and R. W. Kavanagh, Phys. Rev. C **51**, 1624 (1995).
[6] D. Zahnow, C. Angulo, C. Rolfs, S. Schmidt, W. H. Schulte, and E. Somorjai, Z. Phys. A **351**, 107 (1995).
[7] W. R. Nelson, H. Hirayama, and D. O. Rogers, SLAC Report No. 265, 1985.
[8] F. Ajzenberg-Selove, Nucl. Phys. **A490**, 1 (1988).
[9] F. C. Barker, Aust. J. Phys. **22**, 293 (1969).